

Predictability of Large Future Changes in Complex Systems

Didier Sornette^{1, 2, 3} and Wei-Xing Zhou¹

¹*Institute of Geophysics and Planetary Physics, University of California, Los Angeles, CA 90095*

²*Department of Earth and Space Sciences, University of California, Los Angeles, CA 90095*

³*Laboratoire de Physique de la Matière Condensée,*

*CNRS UMR 6622 and Université de Nice-Sophia Antipolis, 06108 Nice Cedex 2, France**

(Dated: October 27, 2019)

We present a systematic algorithm testing for the existence of collective self-organization in the behavior of agents in social systems, with a concrete empirical implementation on the Dow Jones Industrial Average index (DJIA) over the 20th century and on Hong Kong Hang Seng composite index (HSI) since 1969. The algorithm combines ideas from critical phenomena, the impact of agents' expectation, multi-scale analysis and the mathematical method of pattern recognition of sparse data. Trained on the three major crashes in DJIA of the century, our algorithm exhibits a remarkable ability for generalization and detects in advance 8 other significant drops or changes of regimes. An application to HSI gives promising results as well. The results are robust with respect to the variations of the recognition algorithm. We quantify the prediction procedure with error diagrams.

PACS numbers: 89.65.Gh, 05.45.-a, 05.45.Df

I. INTRODUCTION

It is widely believed that most complex systems are unpredictable, with concrete implications in earthquake prediction [1], in engineering failure [2], and in financial markets [3] to cite a few. In addition to the persistent failures of predictive schemes for these systems, concepts such as self-organized criticality [4] suggest an intrinsic impossibility for the prediction of catastrophes. Several recent works suggest a different picture: catastrophes may result from novel mechanisms amplifying their size [5] and may thus be less unpredictable than previously thought. This idea has been mostly explored in material failure [6], in earthquakes [7], and in financial markets and emerged in the latter from the analysis of cumulative losses (drawdowns) [8], from measures of algorithmic complexity [9], and from agent-based models [10].

We present novel empirical tests that provide a strong support for this hypothesis. We focus our analysis on financial indices (typically the daily Dow Jones Industrial Average (DJIA) from 26-May-1896 to 11-Mar-2003) as they provide perhaps the best data sets that can be taken as proxies for other complex systems.

This paper is organized as follows. Section II presents the theoretical foundation of our approach. Section III describes the definition of the pattern recognition method and its implementation and tests on the DJIA. Section IV shows further tests on the Hong Kong Hang-Seng index and section V concludes.

II. THEORETICAL FOUNDATION OF OUR APPROACH

Our key idea is to test for signatures of collective behaviors similar to those well-known in condensed-matter and statistical physics. Collective behaviors in population of agents can emerge through the forces of imitation leading to herding [11]. Herding behavior of investors is reflected in significant deviations of financial prices from their fundamental values [12], leading to so-called speculative bubbles [13] and excess volatility [14]. The similarity between herding and statistical physics models, such as the Ising model, has been noted by many authors [15, 16]. We use it to model a speculative bubble as resulting from positive feedback investing, leading to a faster-than-exponential power law growth of the price [17]. In addition, the competition between such nonlinear positive feedbacks, negative feedbacks due to investors trading on fundamental value and the inertia of decision processes lead to nonlinear oscillations [18] that can be captured approximately by adding an imaginary part to the exponent of the power law price growth. This describes the existence of accelerating log-periodic oscillations obeying a discrete scale invariance (DSI) symmetry [16, 19]:

$$\ln[\pi(t)] = A - B\tau^m + C\tau^m \cos[\omega \ln(\tau) - \phi] , \quad (1)$$

where $\pi(t)$ is the price, ω is the angular log-frequency, $B > 0$ and $0 < m < 1$ for an acceleration to exist, ϕ is an arbitrary phase determining the unit of the time, and $\tau = t_c - t$ is the distance to the critical time t_c defined as the end of the bubble. A statistical analysis of over thirty bubbles and their crashes in the major financial markets shows that the DSI parameter ω exhibits a remarkable universality, with a mean of 6.4 and standard deviation of 1.6 [20], suggesting that it is a significant distinguishing feature of bubble regimes.

*Electronic address: sornette@moho.ess.ucla.edu

This physics-type construction is however missing an essential ingredient distinguishing the natural and physical from the social sciences, namely the existence of expectations: market participants are trying to discount a future that is itself shaped by market expectations. As exemplified by the famous parable of Keynes' beauty contest, in order to predict the winner, recognizing objective beauty is not very important, but knowledge or prediction of others' prediction of beauty is much more relevant. Similarly, mass psychology and investors' expectations influence financial markets significantly. We use the rational-expectation (RE) Blanchard-Watson model of speculative bubbles [21] to describe concisely such feedback loops of prices on agent expectation and vice-versa. Applied to a given bubble price trajectory, agents form an expectation of the sustainability of such bubble and of its potential burst. By this process, to each price $\pi(t)$ is associated a crash hazard rate $h(t)$, such that $h(t)dt$ is the probability for a crash or large change of regime of average amplitude κ to occur between t and $t+dt$ conditioned on the fact that it has yet happened. $h(t)$ quantifies the general belief of agents in the non-sustainability of the bubble. The RE-bubble model predicts the remarkable relationship [17]

$$\ln \left[\frac{\pi(t)}{\pi(t_0)} \right] = \kappa \int_{t_0}^t h(t') dt' \quad (2)$$

linking price to crash hazard rate. Putting (1) in (2) and using the fact, that by definition $h(t) \geq 0$, gives the constraint $b \equiv Bm - |C|\sqrt{m^2 + \omega^2} \geq 0$. This condition has been found to provide a significant feature for distinguishing market phases with bubbles ending with crashes from regimes without bubbles [22].

III. THE PATTERN RECOGNITION METHOD

A. Objects and classes

Let us now build on these insights and construct a systematic predictor of bubble regimes and their associated large changes. Due to the complexity of financial time series, to the existence of many different regimes, and to the constant action of investors arbitraging gain opportunities, it is widely held that the prediction of crashes is an impossible task [23]. The truth is that financial markets do not behave like statistically stationary physical systems and exhibit a variety of non-stationarities, influenced both by exogenous and endogenous shocks [24]. To obtain robustness and to extract information systematically in the approximately self-similar price series, it is useful to use a multiscale analysis: tests of (1) and (2) are thus performed for each trading day over nine different time scales of 60, 120, 240, 480, 720, 960, 1200, 1440 and 1680 trading days.

Each trading day ending an interval of length 1680 or smaller is called an object and there are a total of 27428

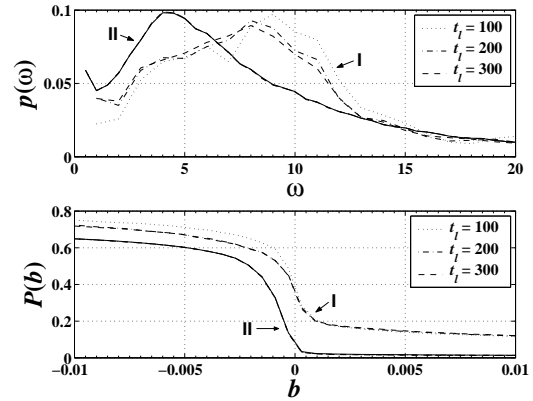


FIG. 1: Density distribution $p(\omega|I \text{ or } II)$ of the DSI parameter ω obtained from (1) and complementary cumulative distribution $P(b|I \text{ or } II)$ of the constraint parameter b obtained from (2) for the objects in classes I (dotted, dashed, and dotted-dashed) and II (continuous) for three different values of t_l .

objects from 06-Feb-1902 till 11-Mar-2003. We define a map from the calendar time t to an ordered index $\$t$ of the trading day, such that $\$t = t$ if t is a trading date and $\$t = \emptyset$ otherwise. We denote $\mathcal{T}_C = \{t_{c,i} : i = 1, \dots, n\}$ a list of targets (crashes) that happened at $t_{c,i}$. All objects are partitioned into two classes I and II, where class $I(t_l) = \{\$t : t_{c,i} - t_l \leq t \leq t_{c,i}, t_{c,i} \in \mathcal{T}_C\}$ contains all the objects in $[t_{c,i} - t_l, t_{c,i}]$ for $i = 1, \dots, n$ and class $II(t_l) = \{T : T = 1, \dots, 27428\} - I$ includes all the remaining, where t_l is a given number in unit of calendar day. In the following, our target set are three well-known speculative bubbles that culminated on 14-Sep-1929, 10-Oct-1987 and 18-Jul-1998, respectively, before crashing in the following week or month.

B. Empirical tests of the relevance of patterns

Figure 1 presents the distributions of the ω 's and b 's obtained from fits with (1) in intervals ending on objects for all time scales and for three different values of t_l . The distributions for classes I and II, which are very robust with respect to changes in t_l , are very different: for $\omega \in [6, 13]$, $p(\omega|I)$ is larger than $p(\omega|II)$; 40% of objects in class I obey the constraint $b \geq 0$ compared to 6% in class II. The very significant differences between the distributions in classes I and II confirm that the DSI and constraint parameters are distinguishing patterns of the three bubbles.

Figure 2 plots a vertical line segment for each time scale at the date t of the object that fulfills simultaneously three criteria: $6 \leq \omega \leq 13$, $b \geq 0$ and $0.1 \leq m \leq 0.9$. The last criterion ensures a smooth super-exponential acceleration. Each stripe thus indicates a potentially dangerous time for the end of a bubble and for the coming of a crash. The number of dangerous objects decreases with

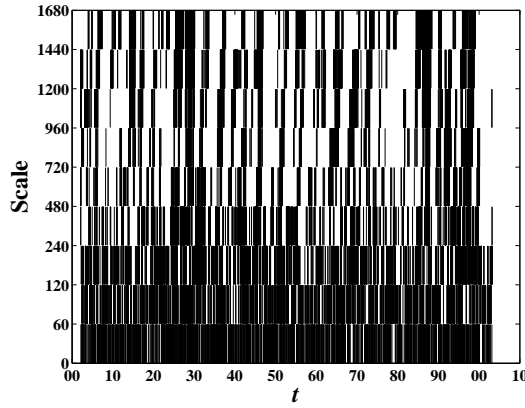


FIG. 2: Alarm times t (or dangerous objects) obtained by the multiscale analysis. The alarms satisfy $b \geq 0$, $6 \leq \omega \leq 13$ and $0.1 \leq m \leq 0.9$ simultaneously. The ordinate is the investigation “scale” in trading day unit. The results are robust with reasonable changes of these bounds.

the increase of the scale of analysis, forming a hierarchical structure. Notice the clustering of alarms, especially at large scales, around the times of the three targets. Altogether, Figs. 1 and 2 suggest that there is valuable information for crash prediction but the challenge remains to decipher the relevant patterns in the changing financial environment. For this, we call in the statistical analysis of sparse data developed by the mathematical Russian school [7, 25] in order to construct a systematic classifier of bubbles. The modified “CORA-3” algorithm [25] that we briefly describe below allows us to construct an alarm index that can then be tested out-of-sample.

Each object is characterized by five quantities, which are believed to carry relevant information: ω , b , m , the r.m.s. of the residuals of the fits with (1) and the height of the power spectrum P_N of log-periodicity at ω [26, 27]. Integrated with the 9 scales, there are totally 5×9 parameters for each object. We set $t_l = 200$ but have checked that all results are robust with large changes of t_l . Class I has 444 objects. By proceeding as in Fig. 1, for each of the 45 parameters, we qualify it as relevant if its distributions in classes I and II are statistically different. We have played with several ways of quantifying this difference and find again a strong robustness. Out of the 45 parameters, 31 are found to be informative and we have determined their respective intervals over which the two distributions are significantly different. We use these 31 parameters to construct a questionnaire of 31 questions asked to each object. The i th question on a given object asks if the value of the i th parameter is within its qualifying interval. Each object A can then be coded as a sequence of binary decisions so that $A = A_1 A_2 \cdots A_{31}$ where A_i is the answer (Y/N) to the i th question.

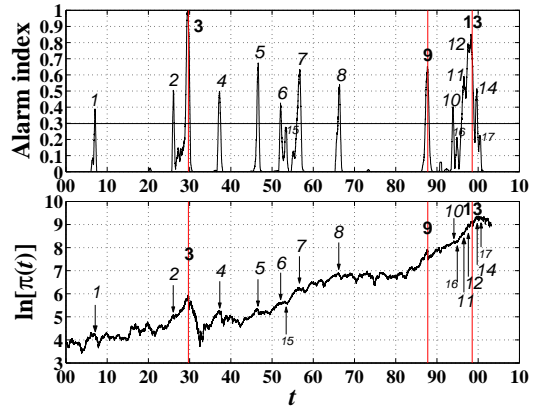


FIG. 3: (Color online) Alarm index $AI(t)$ (upper panel) and the DJIA index from 1900 to 2003 (lower panel). The peaks of the alarm index occur at times indicated by arrows in the bottom panel.

C. Construction of the alarm index and tests on the DJIA

A distinctive property of the pattern recognition approach is to strive for robustness notwithstanding the lack of sufficient training data (here only three bubbles) [25]. In this spirit, we define a trait as an array (p, q, r, P, Q, R) where $p = 1, 2, \dots, 31$, $q = p, p + 1, \dots, 31$, $r = q, q + 1, \dots, 31$ and $P, Q, R = Y$ or N . There are $2^{(31)} + 4^{(31)} + 8^{(31)} = 37882$ possible traits. If $P = A_p$, $Q = A_q$ and $R = A_r$, we say that the object A exhibits a trait (p, q, r, P, Q, R) . The number of questions (three are used here) defining a trait is a compromise between significance and robustness. A feature is a trait that is present relatively frequently in class I and relatively infrequently in class II. Specifically, if there are no less than k_I objects in class I and no more than k_{II} objects in class II that exhibit a same trait, then this trait is said to be a feature of class I. Calling $n(\$t)$ the number of distinctive features of a given object at time t by a voting process, we define the alarm index $AI(t)$, here amounting to perform a moving average of $n(\$t)$ over a time window of width Δ . We then normalize it: $AI(t) \rightarrow AI(t) / \max_t \{AI(t)\}$.

Figure 3 shows the alarm index $AI(t)$ for $\Delta = 100$ with $k_I = 200$ (corresponding to at least 45.1% of the objects in class I) and $k_{II} = 1500$ (corresponding to no more than 5.6% of the objects in class II). The alarm index is found to be highly discriminative as only 13.0%, 9.5%, and 4.7% of the total time is occupied by a high level of alarm larger than 0.2, 0.3, and 0.4 respectively. We have performed extensive experiments to test the robustness of the results. We have varied simultaneously k_I from 100 to 400 with spacing 50 and k_{II} from 1000 to 4000 with spacing 500. The voting results are remarkably robust with no change of the major peaks.

The three bubbles used in the learning process are predicted: peak 3 is on 01-Jul-1929 (market maximum on

14-Sep-1929); peak 9 is on 10-Oct-1987 (market maximum on 04-Sep-1987 and crash on 19-Oct-1987); peak 13 is on 23-Apr-1998 (market maximum on 18-Jul-1998). This timing is a good compromise for a prudent investor to exit or short the market without losing much momentum. This success is however not a big surprise because this corresponds to in-sample training. The most remarkable property of our algorithm is its ability for generalizing from the three bubbles ending with crashes to the detection of significant changes of regimes that may take a large variety of shapes.

The following peaks are predictors of crashes or of strong corrections with an $AI = 0.3$ alarm threshold: peak 1 (Jan, 1907), peak 4 (Apr, 1937), peak 5 (Aug, 1946), peak 6 (Jan, 1952), peak 7 (Sep, 1956), peak 8 (Jan, 1966), peak 12 (Jul, 1997) and peak 14 (Sep, 1999). The more than 20% price drops in 1907 (peak 1) and 1937 (peak 4) have been previously identified as crashes occurring over less than three months [28]. Peak 12 is occurring three months before the turmoil on the stock market (one day 7% drop on 27-Oct-1997) that was followed by a three month plateau (see discussion in Chapter 9 of Ref. [16]). Peak 10 is a false alarm. Peaks 2 and 11 can be regarded as early alarms of the following 1929 crash and 1997, 1998, and 2000 descents. Peak 15-17 are smaller peaks just barely above $AI = 0.2$. Peaks 15 and 16 are false alarms, while peak 17 (31-May-2000) is just two months before the onset of the global anti-bubble starting in August of 2000 [29].

Figure 4 is constructed as follows. Each alarm index peak is characterized by the time t_c of its maximum and by its corresponding log of price $\ln[\pi(t_c)]$. We stack the index time series by synchronizing all the t_c for each peak at the origin of time and by translating vertically the prices so that they coincide at that time. Figure 4 shows four years of the DJIA before and two years after the time of each alarm index maximum. We choose this representation to avoid the delicate and still only partly resolved task of defining what is a crash, a large drop or a significant change of regime. On this problem, the literature is still vague and not systematic. Previous systematic classifications [8, 28] miss events that are obvious to the trained eyes of professional investors or on the contrary may incorporate events that are controversial.

Figure 4 shows that these peaks all correspond to a time shortly before sharp drops or strong change of market regimes. In a real-time situation, a similar prediction quality can be obtained in identifying the peaks by waiting a few weeks for the alarm index to drop or alternatively by declaring an alarm when $AI(t)$ reaches above a level in the range $0.2 - 0.4$. The sharpness and the large amplitudes of the peaks of the alarm index ensures a strong robustness of this latter approach. Our method however misses several large price drops, such as those in 1920, 1962, 1969, 1974 [16, 28]. This may be attributed to a combination of the fact that some large market drops are not due to the collective self-organization of agents but result from strong exogenous shocks, as ar-

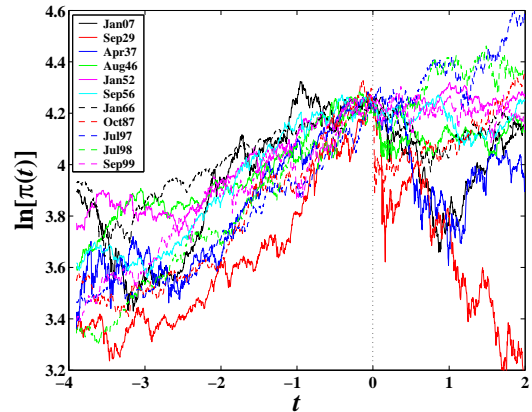


FIG. 4: (Color online) Superposed epoch analysis of the 11 time intervals, each of 6 years long, of the DJIA index centered on the time of the maxima of the 11 predictor peaks above $AI = 0.3$ of the alarm index shown in Fig. 3.

gued in Refs. [20, 24] and that the method needs to be improved. However, the generalizing ability of our learning algorithm strengthens the hypothesis that herding behavior leads to speculative bubbles and sharp changes of regimes.

D. Error diagrams for evaluation of prediction performance

1. Theoretical background

This brief presentation is borrowed from Chap. 9 of the book in [16]. In evaluating predictions and their impact on (investment) decisions, one must weight the relative cost of false alarms with respect to the gain resulting from correct predictions. The Neyman-Pearson diagram, also called the decision quality diagram, is used in optimizing decision strategies with a single test statistic. The assumption is that samples of events or probability density functions are available both for correct signals (the crashes) and for the background noise (false alarms); a suitable test statistic is then sought which optimally distinguishes between the two. Using a given test statistic (or discriminant function), one can introduce a cut which separates an acceptance region (dominated by correct predictions) from a rejection region (dominated by false alarms). The Neyman-Pearson diagram plots contamination (misclassified events, i.e., classified as predictions which are thus false alarms) against losses (misclassified signal events, i.e., classified as background or failure-to-predict), both as fractions of the total sample. An ideal test statistic corresponds to a diagram where the “Acceptance of prediction” is plotted as a function of the “acceptance of false alarm” in which the acceptance is close to 1 for the real signals, and close to 0 for the false alarms. Different strategies are possible: a “liberal” strategy favors minimal loss (i.e., high acceptance

of signal, i.e., almost no failure to catch the real events but many false alarms), a “conservative” one favors minimal contamination (i.e., high purity of signal and almost no false alarms but many possible misses of true events).

Molchan has shown that the task of predicting an event in continuous time can be mapped onto the Neyman-Pearson procedure. He has introduced the “error diagram” which plots the rate of failure-to-predict (the number of missed events divided by the total number of events in the total time interval) as a function of the rate of time alarms (the total time of alarms divided by the total time, in other words the fraction of time we declare that a crash or large correction is looming) [30, 31] (see also [7] for extensions and reviews). The best predictor corresponds to a point close to the origin in this diagram, with almost no failure-to-predict and with a small fraction of time declared as dangerous: in other words, this ideal strategy misses no event and does not declare false alarms! These considerations teach us that making a prediction is one thing, using it is another which corresponds to solving a control optimization problem [30, 31].

2. Assessment of the quality of predictions by the error diagram

To assess quantitatively the prediction procedure described above, we thus construct an error diagram, plotting the failure to predict as a function of the total alarm duration. The targets to be predicted are defined as large drawdowns (cumulative losses as defined in [8]) whose absolute values are greater than some given value r_0 . Each drawdown has a duration covering a time interval $[t_1, t_2]$. For a given alarm index threshold AI_0 , if there exist a time $t \in [t_1 - \Delta t, t_1]$ so that $AI(t) \geq AI_0$, then the drawdown is said to be successfully predicted; in contrast, if $AI(t) < AI_0$ for all $t \in [t_1 - \Delta t, t_1]$, we say it is a failure. This definition ensures that the forecast occurs before the occurrence of the drawdown. The error diagram is obtained by varying the decision threshold AI_0 . The quantity “failure to predict” is the ratio of the number of failures over the number of targets as said above. The total alarm duration is the total time covered by the objects whose alarm index is larger than AI_0 divided by the total time. By varying the value of AI_0 , we obtain different pairs of failure to predict and total alarm duration.

Figure 5 presents the error diagram for two target definitions ($r_0 = 0.1$ and $r_0 = 0.15$) for the DJIA with $\Delta t = 40$, $k_I = 250$ and $k_{II} = 3500$. The anti-diagonal corresponds to the completely random prediction scheme. The error diagrams with different Δt , k_I and k_{II} are found to be similar, with small variations, showing a strong robustness of our construction. The inset shows the prediction gain, defined as the ratio of the fraction of targets correctly predicted (equal to 1 – failure to predict) to the total alarm duration. Theoretically, the prediction gain of a random prediction strategy is 1. The er-

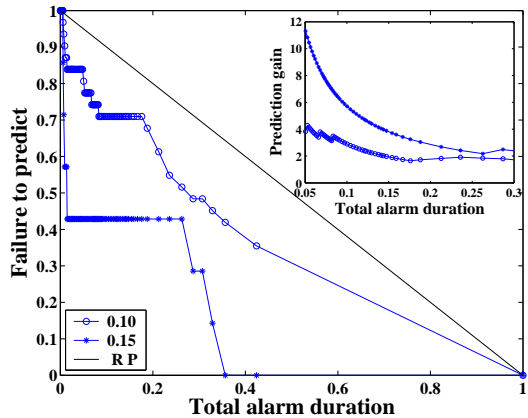


FIG. 5: Error diagram for our predictions for two definitions of targets to be predicted $r_0 = 0.1$ and $r_0 = 0.15$ obtained for the DJIA. The anti-diagonal line corresponds to the random prediction result. The inset shows the prediction gain.

ror diagram shows that half of the targets with $r_0 = 0.15$ are predicted with a very small alarm duration and all targets are predicted for an alarm duration less than 40%. This gives rise to large prediction gains for small alarm durations, confirming the very good quality of our predictors. Confidence in this conclusion is enhanced by finding that the quality of the prediction increases as the targets are evolved toward largest losses (10% loss for $r_0 = 0.1$ to 15% loss for $r_0 = 0.15$). This trend continues for largest losses but there are too few events to draw statistically meaningful conclusions for larger drawdowns of 20% or more.

IV. TESTS ON THE HONG KONG HANG SENG COMPOSITE INDEX (HSI)

The validity of our construction should be ascertained by testing it without modification on other independent time series. Here, we present similar promising results obtained for the Hong Kong Hang Seng composite index (HSI) from 24-Nov-1969 to present. The Hong Kong Hang Seng composite index is particularly interesting as it can be considered as a “textbook” example of an unending succession of bubbles and crashes [32]. The nine biggest crashes since 24-Nov-1969 were triggered approximately at the following dates: 20-Sep-1971, 5-Mar-1973, 04-Sep-1978, 13-Nov-1980, 01-Oct-1987, 15-May-1989, 4-Jan-1994, 8-Aug-1997, and 28-Mar-2000. Except for the last one which was posterior to the study published in [32], all of them have been studied previously in [32]. The distinctive properties of the first eight bubbles are consistent with those reported previously [32] (see page 461 concerning the parameters ω and m). In contrast with Ref. [32] in which the positivity constraint was not considered, we find here that it plays a significant role in screening out solutions. We use the two crashes in 1987 and 1997 to train the parameters of our algorithm be-

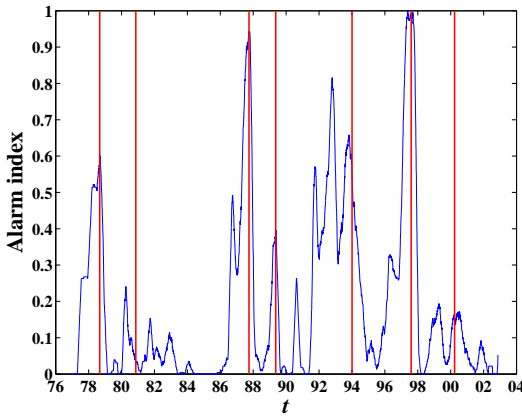


FIG. 6: (Color online) Alarm index $AI(t)$ constructed by our algorithm for the Hong Kong Hang Seng composite index since 24-Nov-1969. The vertical lines indicate the timing of the seven crashes that have not been used in the training part [33].

cause they give the best defined log-periodic power law patterns over the longest time intervals.

Figure 6 illustrates the typical result for the Alarm Index obtained with $t_l = 200$, $k_I = 210$ and $k_{II} = 1700$. Four out of the five crashes that were not used in the training phase are identified very clearly by the alarm index peaks (note that the first two crashes in 20-Sep-1971 and 5-Mar-1973 are omitted in our counting since they occur before the time when our Alarm Index can be constructed). This encouraging result seems to confirm the hypothesis that the seven crashes, posterior to 1976 where the Alarm Index can be defined, are triggered by endogenous stock market instabilities preceded by log-periodic power-law speculative bubbles [20]. Varying the values of the parameters t_l , k_I and k_{II} of our algorithm gives results which are robust.

In addition, one can identify more peaks in Fig. 6 and it is an interesting question to test whether they are associated with an anomaly in the market. In total, we count 15 peaks in Fig. 6 around 15-Sep-1978 (S), 09-Apr-1980 (?), 29-Sep-1981 (F), 30-Nov-1982 (F), 01-Oct-1986 (?), 30-Sep-1987 (S), 20-May-1989 (S), 18-Aug-1990 (F), 09-Oct-1991 (F), 19-Oct-1992 (F), 28-Oct-1993 (S), 05-May-1996 (?), 06-Aug-1997 (S), 10-Apr-1999 (F), and 25-Mar-2000 (S), whose alarm indexes are greater than 0.1. Six peaks whose dates are identified by “S” correspond to successful predictions, among which two are trivial since they were used in the training process. Six peaks identified with “F” are false alarms. The remaining three peaks marked with “?” are neither successful predictions nor complete false alarms as they fall close to crashes. The date with an alarm index of 0.1 on the east side of the first “?” alarm peak is 31-Jul-1980 and can probably be interpreted as a forerunner of the crash on 13-Nov-1980. The two other “?” alarm peaks can probably be interpreted as “fore-alarms” of two main alarm peaks used for training the algorithm.

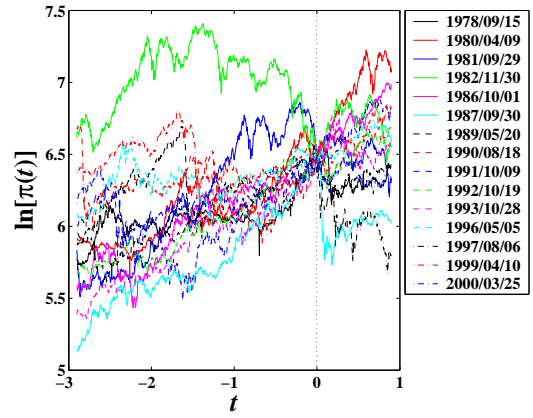


FIG. 7: (Color online) Superposed epoch analysis of the 15 time intervals of the HSI index centered on the time of the maxima of the 15 peaks above $AI = 0.1$ of the alarm index shown in Fig. 6.

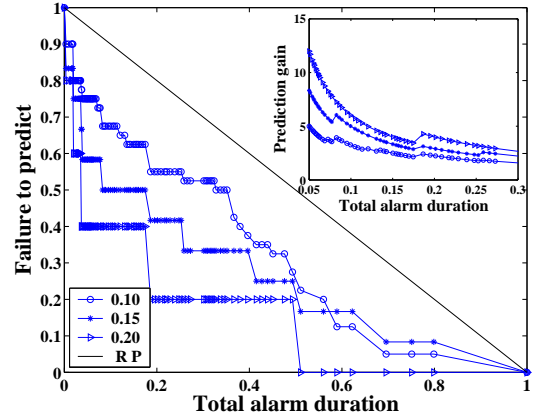


FIG. 8: Error diagram of the predictions for three definitions of targets to be predicted with $r_0 = 0.1$, $r_0 = 0.15$, and $r_0 = 0.2$ in regard to HSI. The diagonal line is a random prediction. In the inset shows the prediction gains.

Similar to Fig. 4, Fig. 7 shows a superposed epoch analysis of the price trajectories a few years before and one year after these 15 peaks, to see whether our algorithm is able to generalize beyond the detection of crashes to detect changes of regimes. The ability to generalize is less obvious for the Hang-Seng index that it was for the DJIA shown in Fig. 4.

Figure 8 presents the error diagram for three target definitions ($r_0 = 0.1$, $r_0 = 0.15$, and $r_0 = 0.2$) for the HSI with $\Delta t = 40$, $k_I = 210$ and $k_{II} = 1700$. The anti-diagonal corresponds to the random prediction scheme. Again, the error diagrams with different Δt , k_I and k_{II} are robust. The results are associated with a very significant predictability and strong prediction gains for small alarm durations.

V. CONCLUDING REMARKS

We find that different stock markets have slightly different characteristics: for instance, the parameters trained on the DJIA are not optimal for the Hang-Seng index. When we use the parameters obtained from the training of our algorithm on the DJIA on the HSI, we find that two of the seven crashes in the HSI are identified accurately (01-Oct-1987 and 4-Jan-1994) while the five other crashes are missed. Interestingly, these two crashes are the most significant. This suggests the existence of a universal behavior only for the “purest” event cases, while smaller events exhibit more idiosyncratic behavior. As we have shown, training our algorithm on these two events on the HSI improves very significantly the prediction of the other events. This shows both a degree of universality of our procedure and the need to adapt to the idiosyncratic structure of each market. This situation is similar to that documented in earthquake predictions

based on pattern recognition techniques [7].

In summary, we have developed a multiscale analysis on the analysis of stock market bubbles and crashes. Based on a theory of investor imitation, we have integrated the log-periodic power-law patterns characteristic of speculative bubbles preceding financial crashes within a general pattern recognition approach. We have applied our approach to two financial time series, DJIA (Dow Jones Industrial Average) and HSI (Hang-Seng Hong Kong index). Training our algorithm on only a few crashes in each market, we have been able to predict the otherwise crashes not used in the training set. Our work provides new evidence of the relevance of log-periodic power-law patterns in the evolution of speculative bubbles supporting the imitation theory.

We are grateful to T. Gilbert for helpful suggestions. This work was partially supported by the James S. Mc Donnell Foundation 21st century scientist award/studying complex system.

[1] See the contributions in *Nature* debates on earthquake prediction, helix.nature.com/debates/earthquake/.

[2] W.J. Karplus, *The Heavens are Falling: The Scientific Prediction of Catastrophes in Our Time* (Plenum Press, New York, 1992).

[3] E.F. Fama, *J. Fin. Econ.* **49**, 283 (1998).

[4] P. Bak, *How Nature Works* (Copernicus, New York, 1996).

[5] D. Sornette, *Phys. World* **12**, 57 (1999); *Proc. Nat. Acad. Sci. USA* **99**, 2522 (2002); V.S. L'vov *et al.*, *Phys. Rev. E* **63**, 056118 (2001).

[6] J.-C. Anifraní *et al.*, *J. Phys. I France* **5**, 631 (1995); A. Garcimartin *et al.*, *Phys. Rev. Lett.* **79**, 3202 (1997); A. Johansen and D. Sornette, *Eur. Phys. J. B* **18**, 163 (2000).

[7] V.I. Keilis-Borok and A.A. Soloviev, eds., *Nonlinear Dynamics of the Lithosphere and Earthquake Prediction* (Springer, Heidelberg, 2003).

[8] A. Johansen and D. Sornette, *Eur. Phys. J. B* **1**, 141 (1998); *J. Risk* **4**, 69 (2001).

[9] R. Mansilla, *Physica A* **301**, 483 (2001).

[10] D. Lamper *et al.*, *Phys. Rev. Lett.* **88**, 017902 (2002).

[11] D. Scharfstein and J. Stein, *Am. Econ. Rev.* **80**, 465 (1990); T. Lux, *J. Roy. Econ. Soc.* **105**, 881 (1995); J.R. Graham, *J. Fin.* **54**, 237 (1999).

[12] R.J. Shiller, *Irrational Exuberance* (Princeton University Press, Princeton, 2000).

[13] R.P. Flood and P.M. Garber, *Speculative Bubbles, Speculative Attacks and Policy Switching* (MIT Press, Cambridge, 1994).

[14] R.J. Shiller, *Market Volatility* (MIT Press, Cambridge, 1989).

[15] E. Callen and D. Shapero, *Phys. Today* **27**, 23 (1974); E.W. Montroll W.W. and Badger, *Introduction to Quantitative Aspects of Social Phenomena* (Gordon and Breach, New York, 1974); A. Orléan, *J. Econ. Behav. Org.* **28**, 257 (1995); A. Krawiecki *et al.*, *Phys. Rev. Lett.* **89**, 158701 (2002).

[16] D. Sornette, *Why Stock Markets Crash* (Princeton University Press, Princeton, 2003); *Phys. Rep.* **378**, 1 (2003).

[17] A. Johansen *et al.*, *J. Risk* **1**, 5 (1999); *Int. J. Theor. Appl. Fin.* **3**, 219 (2000); D. Sornette and J.V. Andersen, *Int. J. Mod. Phys. C* **13**, 171 (2002).

[18] K. Ide and D. Sornette, *Physica A* **307**, 63 (2002).

[19] D. Sornette, *Phys. Rep.* **297**, 239 (1998).

[20] A. Johansen and D. Sornette, cond-mat/0210509; A. Johansen, *Physica A* **324**, 157-166 (2003).

[21] O.J. Blanchard, *Econom. Lett.* **3**, 387 (1979); O.J. Blanchard and M.W. Watson, In: P. Wachtel (Ed.), *Crisis in Economic and Financial Structure: Bubbles, Bursts, and Shocks* (Lexington Books, Lexington, 1982).

[22] H.-C. Bothmer and C. Meister, *Physica A* **320**, 539 (2003).

[23] A. Greenspan, Economic Volatility, Remarks at symposium sponsored by the Federal Reserve Bank of Kansas City, Jackson Hole, Wyoming, August 30, 2002.

[24] D. Sornette *et al.*, *Risk* **16**, 67 (2003).

[25] I.M. Gelfand *et al.*, *Phys. Earth Planet. Inter.* **11**, 227 (1976).

[26] W. Press *et al.*, *Numerical Recipes in Fortran* (Cambridge University, Cambridge, 1996);

[27] W.-X. Zhou and D. Sornette, *Int. J. Mod. Phys. C* **13**, 137 (2002).

[28] F.S. Mishkin and E.N. White, NBER Working Paper No. 8992, www.nber.org/papers/w8992.

[29] D. Sornette and W.-X. Zhou, *Quant. Fin.* **2**, 468 (2002); W.-X. Zhou and D. Sornette, cond-mat/0212010; physics/0301023.

[30] G.M. Molchan, *Physics of the Earth and Planetary Interiors* **61**, 84-98 (1990).

[31] G.M. Molchan, *Pure and Applied Geophysics* **149**, 233-247 (1997).

[32] D. Sornette and A. Johansen, *Quant. Fin.* **1**, 452 (2001).

[33] The first two crashes are not included in the analysis since the longest window used in our multiscale analysis is seven years.